Autonomous Underwater Vehicle Model-Based High-Gain Observer for Ocean Current Estimation

Eonjoo Kim
Australian Maritime College
University of Tasmania
Launceston, Tasmania, Australia
eonjook@utas.edu.au

Shuangshuang Fan
Australian Maritime College
University of Tasmania
Launceston, Tasmania, Australia
Department of Ocean and Naval Architectural Engineering
Memorial University of Newfoundland
St. John's, Newfoundland, Canada
shuangshuang.fan@utas.edu.au

Neil Bose
Department of Ocean and Naval Architectural Engineering
Memorial University of Newfoundland
St. John's, Newfoundland, Canada
Australian Maritime College
University of Tasmania
Launceston, Tasmania, Australia
nbose@mun.ca

***Abstract*—Autonomous Underwater Vehicles (AUVs) are being used as specialised tools for various ocean missions, and there are advantages in applying more accurate dynamic models for control. In this study, a high-gain observer (HGO) based on an AUV dynamics model is presented to estimate three-dimensional water current velocities. The water current velocities were determined by calculating the differences between the vehicle's absolute velocities and the relative velocities estimated by the model-based HGO. The HGO was chosen as a nonlinear algorithm to estimate the vehicle's relative velocities. The Lyapunov stability of the estimation error dynamics was investigated. The observer gain was computed by solving the Linear Matrix Inequality (LMI) which represented the error dynamics. By utilising the AUV model-based HGO, the vehicle's relative velocity was estimated, then the current velocity vector was subsequently calculated. AUV numerical simulations and field test results were used to confirm the effectiveness of the proposed HGO, and the improvements over previous solutions.**

Keywords— Autonomous Underwater Vehicles; Model-aided inertial navigation; High-gain observer; Nonlinear observer; Linear Matirx Inequality.

I. INTRODUCTION

AUVs have drawn attention over the past decades through their use for various ocean missions such as seabed mapping and observations, environmental monitoring and oceanographic measurements. These tasks involve high-resolution, georeferenced optical/acoustic ocean floor mapping as well as water column sampling such as currents, temperature and salinity [1]. Georeferencing is critical for AUVs to register navigational information and to revisit a previous mission site. One of the major challenges is to achieve accurate localisation and navigation in regions where a Doppler Velocity Log (DVL) is out of range of the bottom [2]. To localise and navigate AUVs, Inertial Navigation Systems (INS) are one of the essential components. The INS estimates the position, orientation and velocity of the vehicle relative to the inertial frame by utilising an Inertial Measurement Unit (IMU). Although a relatively large position error drift results in a navigation system based solely on an INS, this error can be reduced by an externally aided bottom tracking DVL [3]. However, DVL aiding is either intermittently or completely unavailable when the vehicle-to-seabed distance is greater than the transmission range of the DVL and this varies with its acoustical frequency: for instance, 300 kHz DVLs have a maximum range of around 200 m, while the maximum range of 1200 kHz DVLs is around 30 m for Teledyne RD Marine DVLs. When the DVL is out of the range of the seabed, the vehicle's velocity can be estimated by utilising a model-based integration navigation algorithm: i.e. a model-aided INS [4]. Despite the fact that the localisation by the model-aided INS is not as precise as the DVL-aided INS, the model-aided INS is more accurate than an unaided INS and the DVL-aided INS in the water tracking mode [5].

The capability of a model-based observer for predicting AUV velocity depends on the accuracy of the parameters representing the hydrodynamic, hydrostatic, environmental and external forces and the mass properties of the AUV. In [6], it was assumed that the flow dynamics was composed of two components– a steady, nonuniform component and an unsteady and uniform component. Based on this assumption, a dynamic model for the motion of a rigid vehicle in an unsteady nonuniform flow was presented in [7]. A nonlinear observer based on a dynamic motion model in a current for an AUV was introduced in [8]. The current velocities were the difference between the vehicle's absolute velocities and relative velocities obtained by the nonlinear observer. The observer gain matrix for this HGO was preliminarily optimised by using the pole placement which appoints the Eigen values at certain poles. There are numerous introduced estimator approaches, but the HGO is the most prominent estimation technique used in nonlinear control [9].

A HGO employs the selection of adequately large gain to reduce the impact of uncertainty and nonlinearity in the error estimation dynamics. However, as the gain becomes higher increased peaking occurs in the transients which destabilizes the control loop [10].The issue of selecting a high gain arises from the demand to account for the nonlinearities in the error dynamics which are typically represented as a Lipschitz function. Alessandri and Rossi [11] presented a time-varying increasing-gain observer for a nonlinear system. In the first time instant, the gain was small, but it increased over time up to its maximum and then was kept constant. The selection of design parameters were produced by solving a set of linear matrix inequalities (LMIs) and a nonlinear programming problem in a few variables. LMI theory has recently gained attention since a wide variety of control problems can be

reduced to a few standard convex optimization problems including LMIs. The form of an LMI is very general, so various constraints from control theory such as Lyapunov and Riccati inequalities can all be written as LMI. Thus, LMIs are a useful tool for solving a wide variety of optimisation and control problems [12]. LMI was adapted in this paper to obtain the gain for the observer design.

This paper presents a nonlinear observer based on an AUV dynamic model in currents to estimate the current velocity. This paper is organised as follows: Section II is devoted to describing the methodology including the AUV kinetic, dynamic models and observer design. Results are presented in Section III and Conclusions in Section IV.

II. METHODOLOGY

The water current velocity can be obtained from the difference between the vehicle's absolute and relative velocity and Equation (1) gives this calculation in vector form.

$$\vec{v}_{\text{current}} = \vec{v}_{\text{Abs}} - \vec{v}_{\text{Rel}} \tag{1}$$

where $\vec{v}_{\text{current}}$ is the current velocity vector ; $\vec{v}_{\text{Abs}}$ is the vector of the vehicle's absolute velocity over the ground; and $\vec{v}_{\text{Rel}}$ is the vector of vehicle's relative velocity through the water estimated by the AUV dynamic model-based observer. In this study, the current components close to the AUV were obtained in 3-principal directions by using the AUV dynamic model-based HGO.

A. Kinematics

In order to analyse the motion of the AUV, two coordinate frames, an inertial reference frame and a body-fixed frame, are defined as shown in Fig. 1 – this is based on the notation from [8]. The inertial frame $\{x_i, y_i, z_i\}$ is fixed in inertial space such that z_i is aligned with the force due to gravity. The vector x_b in the body-fixed reference frame is aligned with the longitudinal axis of the vehicle while vector y_b is directed to port and z_b is directed to the bottom.

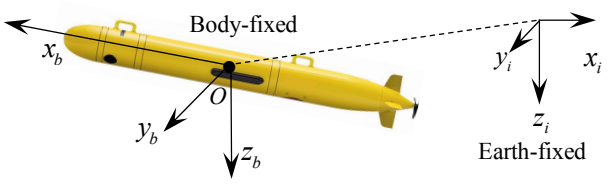

Fig. 1 AUV's body-fixed and earth-fixed reference frames.

$X = [x, y, z]^{\mathrm{T}}$ is the position vector from the origin of the inertially fixed frame to the origin of body-fixed reference frame. The vector X is in North-East-Down coordinates and is described in the inertial frame. The vehicle's translational and rotational velocities are denoted as $\upsilon = [u, v, w]^{\mathrm{T}}$ and $\omega = [p, q, r]^{\mathrm{T}}$ with respect to the inertial frame, but they are represented in the body frame of reference. The kinematic equations are

$$\begin{aligned} \dot{x} &= R\nu \\ \dot{R} &= R\hat{\omega} \end{aligned} \tag{2}$$

where $\hat{\cdot}$ denotes the 3×3 skew-symmetric matrix satisfying $\hat{a}b = a \times b$ for vectors a and b.

Based on the theory in [13], a current flow $V_f(X, t)$ consists of an unsteady, uniform flow component $V_u(t)$ and a steady, circulating flow component $V_s(\mathrm{X})$. In the body-fixed reference frame, two flow components are more favorably represented as Equation (3). Then the flow field can be represented by summing these two components as Equation (4).

$$\begin{aligned} v_u(R,t) &= R^T V_u(t) \\ v_s(R,X) &= R^T V_s(X) \end{aligned} \tag{3}$$

$$v_f(R,X,t) = v_u(R,t) + v_s(R,X) \tag{4}$$

B. Dynamics

Referring to [14] and [15], the dynamic equations of an AUV in currents can be derived in terms of the flow-relative velocity as shown in Equation (5), and the explanation of these terms is not elaborated here for reasons of brevity.

$$\begin{aligned} (M_f + M)\dot{\nu}_r = & \\ & -\begin{pmatrix} \hat{\omega} & 0 \\ \hat{v}_r & \hat{\omega} \end{pmatrix}(M_f + M)\nu_r + \begin{pmatrix} f \\ m \end{pmatrix} \\ & -\begin{pmatrix} \hat{\omega} & 0 \\ \hat{v}_r + \hat{v}_u + \hat{v}_s & \hat{\omega} \end{pmatrix}(M - \bar{M})\begin{pmatrix} v_u + v_s \\ 0 \end{pmatrix} \\ & -\begin{pmatrix} 0 & 0 \\ \hat{v}_u + \hat{v}_s & 0 \end{pmatrix}(M - \bar{M})\nu_r - \begin{pmatrix} \Phi & 0 \\ 0 & 0 \end{pmatrix}(M_f + \bar{M})\nu_r \\ & -(M - \bar{M})\begin{pmatrix} (v_u + v_s)\omega + \dfrac{\partial}{\partial t}v_u + \Phi^T(v_u + v_s + v_r) \\ 0 \end{pmatrix} \end{aligned} \tag{5}$$

C. Observer Design based on AUV dyanmics in currents

This section is devoted to establishing the HGO based on a dynamic model in a current for the AUV in order to obtain the current velocity estimate. By using the kinematic equation (2) and dynamic equation (5), the system dynamics can be express as

$$\begin{aligned} \dot{x} &= Ax + f(x,u,d) \\ y &= Cx \end{aligned} \tag{6}$$

where $x(t)=[\varphi, \theta, \psi, u_r, v_r, w_r, p, q, r]^{\mathrm{T}}$ is the state vector; and $u=[n, \delta_r, \delta_e]^T$ is the control input. The term n stands for the propeller's rotation and δ_r, δ_e are the deflection of the rudder and elevators respectively. The term d denotes disturbances caused by the current; y is the output vector; and C represents the measurement matrix [8].

It is usual to measure Euler angles by an electronic compass or an INS. Also, an AUVs absolute velocity is directly sensed by using DVL or indirectly achieved by position differentiation. The DVL can measure the vehicle's relative velocity to the flow, but the result is less accurate since the DVL can only lock the water column some distance away from the vehicle body, caused by the DVL blanking distance. So, here it is assumed that the relative velocity of the AUV to the fluid is not measurable. The observer was designed using the measurement of output y as follows:

$$\dot{\hat{x}} = A\hat{x} + \hat{f}(\hat{x},u) + G(\gamma,K)(y - C\hat{x}) \tag{7}$$

where $\hat{x}(t) \in \mathbb{R}^n$ is the estimate of $x(t)$; observer gain, $G(\gamma,K):=[\ \gamma k_1\ \gamma^2 k_2\ \ldots\ \gamma^n k_n]^T$ with $K:=[k_1\ k_2\ \ldots\ k_n]^T$,$k_i \in \mathbb{R}$ and i = 1, 2, …, n [16]. Since f is a known function of $f(x, u)$ it is taken that $\hat{f} = f$. From Equations (6) and (7), the estimation error $(\hat{e} := x - \hat{x})$ dynamics were derived as follows:

$$\dot{\hat{e}}(t) = (A - GC)\hat{e}(t) + f(x(t),t) - \hat{f}(x(t) - \hat{e}(t),t) \qquad (8)$$

The stability of the error dynamics was investigated via a Lyapunov function. Furthermore, since (A, C) is observable, there exist λ>0, $K \in \mathbb{R}^n$ and a symmetric positive matrix $P \in \mathbb{R}^{n\times n}$ such as in Equation (9) which could be treated by solving the equivalent LMI as expressed in Equation (10).

$$(A - KC)^{\mathrm{T}} P + P(A - KC) + \lambda I < 0 \qquad (9)$$

$$A^{\mathrm{T}}P + PA - C^{\mathrm{T}}Y^{\mathrm{T}} - YC + \lambda I < 0 \qquad (10)$$

where the unknowns are $\lambda > 0$, $Y=PK \in \mathbb{R}^n$ and $P>0$.

To compute the solution to a given system of LMIs, a number of MATLAB functions were used. Before starting the description of a new LMI system, a function `setlmis` was used to initialise its internal representation. The function `limvar` defined new matrix variables P, Y and λ in the LMI system currently described. The variable matrix P was defined as a 9×9 symmetric matrix while Y was defined as a 3×3 rectangular matrix. One of the gain parameters, λ was defined as a constant. By using a function `limterm`, a term can be added in the LMI system currently specified. The LMI term refers to the elementary additive terms involved in the block-matrix expression of the LMI. More details for the `lmiterm` function description, see [17]. After completing the description of a given LMI system with `lmivar` and `lmiterm`, its internal representation `lmisys` was obtained with the command `getlmis`. The function `feasp` was used to compute a solution `xfeas` of the system of LMIs descripted by `lmisys`. The vector `xfeas` is a value of the decision variables for which all LMIs are satisfied. Finally, a function `dec2mat` computed the corresponding value `valx` of the matrix variable with identifier X given the value `decvars` of the vector of decision variables. As a results, matrix variables - P,Y and λ in the LMI system were obtained, then P and Y were used to calculate the gain parameter K [18]. The high-gain observer design was accomplished by solving the LMI problem so the gain $K=P^{-1}Y$ and γ were obtained as follows:

$$\gamma = 2.7408, \quad K = \begin{bmatrix} 2.2616 & 0 & 2.8609 \\ 0 & 1.6410 & 0 \\ -0.7642 & 0 & 2.1939 \\ 0 & 0.1007 & 0 \\ -0.2669 & 0 & -0.9479 \\ 0 & 0.5343 & 0 \\ -9.9621 & 0 & 4.3196 \\ 0 & 1.7590 & 0 \\ 2.5424 & 0 & 4.1070 \end{bmatrix}$$

III. Results and Discussion

This section describes the validation of the proposed HGO by numerical simulations and experimental field tests.

A. Numerical Simulation

The AUV model applied in this simulation is outlined in reference [19]. The AUV of this model has a prolate spheroid hull shape, is 1.33-meter-long with a fitness ratio of 7:1. The propeller is fixed so that the nominal speed is greater than zero. The attitude of the AUV is controlled by the rudder and elevators through proportional- derivative (PD) feedback [8]. It is assumed that the AUV operated in a nonuniform flow expressed as:

$$V_f(X) = [-0.4, -0.3\sqrt{1 + x/500}, 0]^T \qquad (11)$$

The AUV was simulated to accomplish a zigzag path from the starting point northwards in the horizontal plane. The heading reference is shift from $\psi = 15°$ to $\psi = -15°$ every 100 seconds. The vehicle departs at $X = [-500, 0, 0]^T$ with original orientation of $\varphi = \theta = \psi = 0°$. The horizontal trajectories resulted from two scenarios: with and without current disturbance. They are illustrated in Fig. 2.

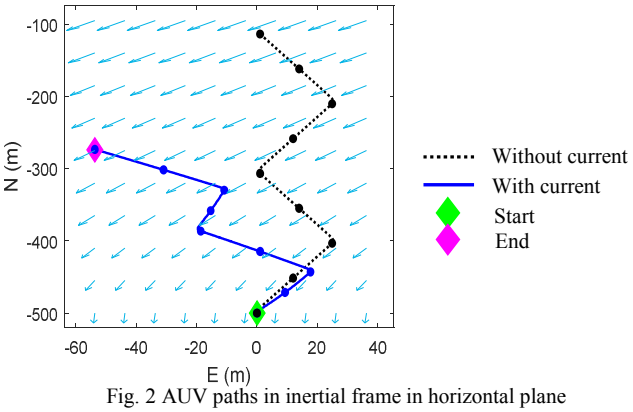

Fig. 2 AUV paths in inertial frame in horizontal plane

There is a significant discrepancy between the two trajectories which resulted from the disrupted vehicle's absolute velocity as a result of the current. In Fig. 3, it can be seen that the vehicle's absolute velocities were affected by the current. While the longitudinal absolute and relative velocitys, u and u_r are nearly even at 0.6 m/s and 1 m/s respectiavely, the lateral absolute speed, v fluctuates as the vehicle changed its heading, thus putting it into a cross current situation.

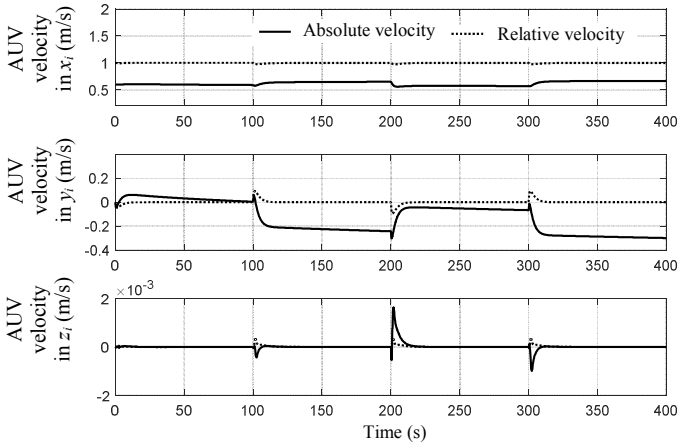

Fig. 3 Vehicle's absolute and relative velocities in x_b, y_b and z_b axes in the body frame reference

The AUV's velocities relative to the flow were estimated by the HGO which utilized the measurement of Euler angles as shown in Fig. 4. The relative velocity estimates generally show agreement with the actual relative velocities, although a peaking phenomenon exists in the transient behavior.

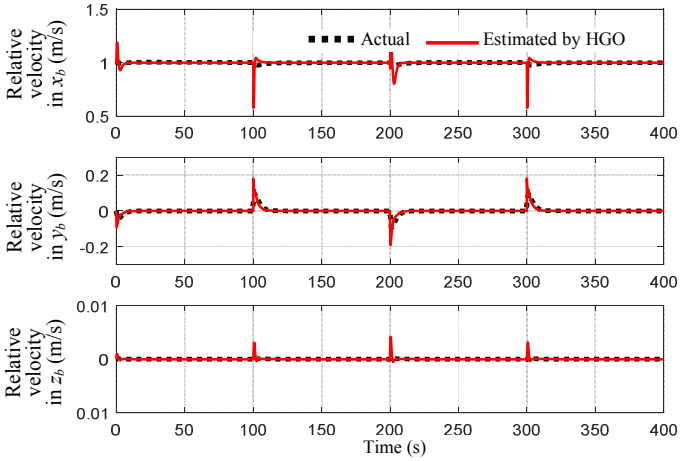

Fig. 4 Comparision between actual and estimated relative velociteis in the x_b, y_b and z_b axes in the body frame reference

Once the vehicle's relative velocities are estimated by using the HGO, then the current velocities can be obtained by subtracting the vehicle's relative velocities from the absolute velocities. It was assumed that the absolute velocities of the vehicle are available with the DVL in operation. As shown in Fig. 5, current velocities in the x_i, y_i and z_i axes in the inertial referenence frame were estimated and these generally matched the actual current.

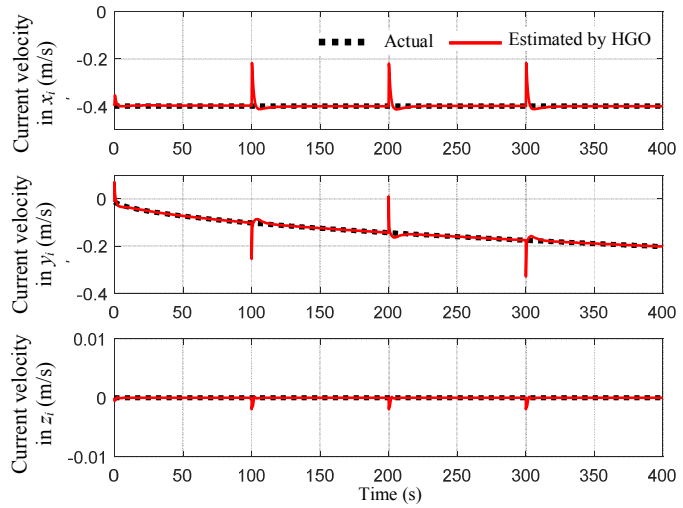

Fig. 5 Comparision between actual and estimated current velociteis in the x_i, y_i and z_i axes in the body frame reference

In order to investigate effectiveness of the HGO using the LMI, current velocity estimates from both the HGO using the LMI and the HGO using the pole placement to generate observer gain [8] were compared as shown in Fig. 6. Estimated current velocity in the x_i axis clearly shows that the HGO using the LMI can estimate current velocity with a lower peaking phenomenon than the pole placement method. The differences between the actual current velocity and the estimated current velocity from the LMI approach are represented by standard deviations of 0.0128 m/s, 0.0038 m/s and 0.0001 m/s while their counter parts using the pole placement method are 0.0285 m/s, 0.0070 m/s and 0.0002 m/s in the x_i, y_i and z_i axes in the body frame reference system respectively.

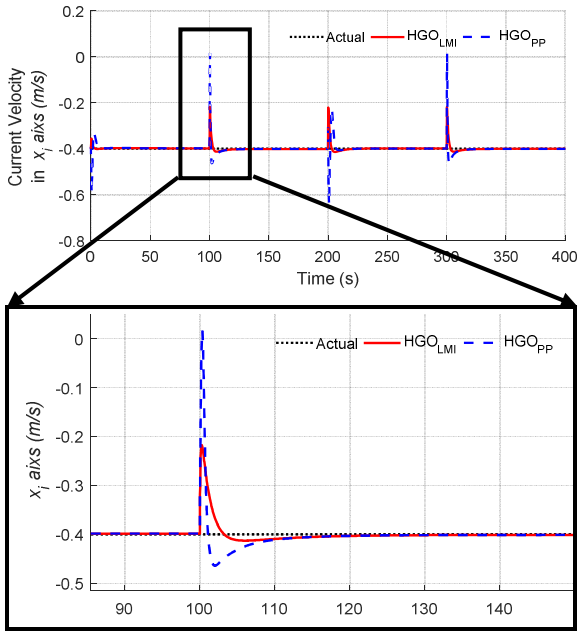

Fig. 6 Comparision between current velocity estimates in the x_i axis in the inertial frame from both HGO and observer using pole placement

Furthermore, an estimation error ratio was calculated according to Equation (13) to see the improvement of the proposed HGO using the LMI to estimate the current velocity compared with HGO using the pole placement method.

$$Estimation\ error\ (\%) = (V_{Act} - V_{Est}) / V_{Act} \times 100 \qquad (12)$$

where V_{Act} is the actual current velocity and V_{Est} is the estimated current by observer. The current estimation errors of HGO using the LMI are considerably less than counter parts of the pole placement method in x_i and y_i axes shown in Fig. 7.

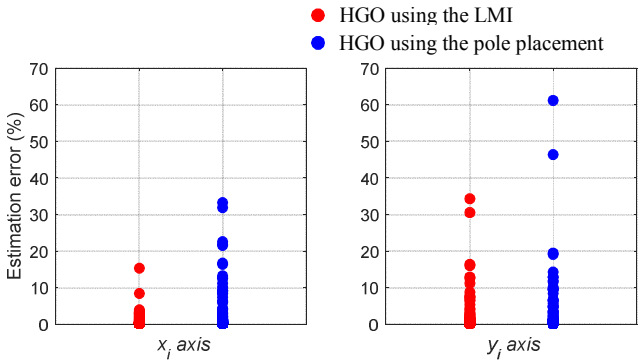

Fig. 7 Estimation error distributions of two observers for current velocity estimates in x_i axis (LEFT) and y_i axis (RIGHT) in the inertial reference frame.

In TABLE I, estimation error means from the current estimation results for the HGO using the LMI and the pole

placement method are tabulated. The estimation error means of the HGO using the LMI are smaller than the pole placement method in both x_i and y_i axes, which results in an estimation improvement of 45 % and 1% respectively.

TABLE I ESTIMATION ERROR MEAN FOR HGO AND OBSERVER USING POLE PLACEMENT

Estimates error mean of	x_i axis	y_i axis
HGO using the LMI	0.6217 %	1.5666%
HGO using the pole placement	1.2187 %	1.5833 %
Estimation improvement of HGO using the LMI	***44.92 %***	***1.05 %***

B. Experimental test

The proposed HGO design was validated through field tests by comparing the estimated current velocities with recorded current velocities from an on-board ADCP. A Gavia-class modular AUV was used for the field tests. Its dimensions were overall length 2.7 m, diameter 0.2 m, and dry weight in air approximately 70 kg [20]. During the field tests, the AUV underwent a straight-line, constant altitude mission at 10 m depth as illustrated in Fig. 8. The water current velocities were measured through the onboard ADCP.

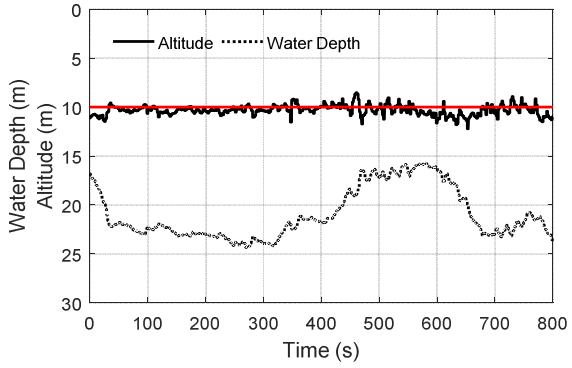

Fig. 8 Water Depth and AUV's altitude during the field test

In order to estimate the current velocities, firstly the vehicle's relative velocities through the water were estimated by the dynamic model-based high-gain observer. Then the current velocities could be calculated by subtracting the estimated relative velocities through the water from the vehicle's absolute velocities over the ground measured by the DVL.

Fig. 9 shows the vehicle's velocities recorded by the DVL-aided INS navigation system during the field test and the vehicle's relative velocities estimated by the HGO in only the x_i direction are presented here due to space. In x_i direction, the vehicle's absolute velocity and relative velocity showed the greatest difference compared to the two other axes, which showed that current velocity in the longitudinal direction was dominant. The straight line that the vehicle followed during the field test was close to inline and against the tidal flow direction.

Fig. 10 shows the current velocities estimated by the HGO and measured current velocities from the ADCP in the x_i axis in the inertial frame. Although the current velocities were measured away from the vehicle due to the ADCP's blanking distance, the estimated current velocities from the observer are closely matched with the measured current velocities. A peaking phenomenon was noted in the estimated current velocity. In the HGO, the peaking phenomenon shows an estimation gap during the short period right after the start of the test. However, the transient period shown in the estimated current velocity was very short relative to the time scale, and the estimated velocity approached the measured current velocity very closely.

In order to investigate the differences between the current velocity estimates from the HGO and the current velocities measured by the ADCP, the standard deviations between these two were quantified as 0.0942 m/s, 0.0656 m/s, and 0.0323 m/s in the x_i, y_i and z_i axes of the inertial reference frame. The current measurement from the ADCP were taken 0.44m away from the vehicle while the current estimates from the observer were calculated at the vehicle.

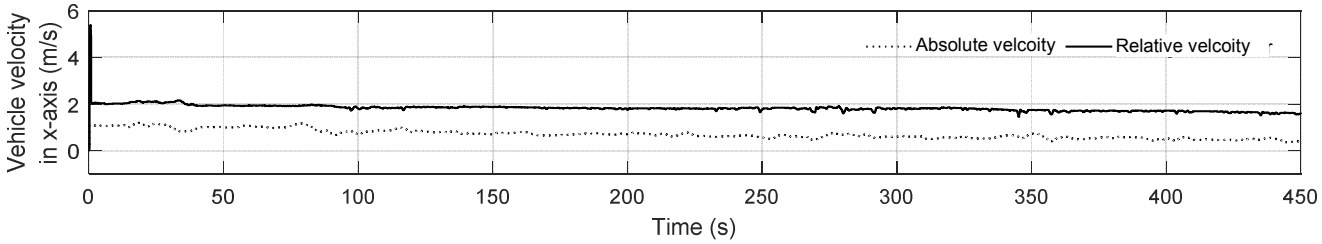

Fig. 9 The vehicle's absolute velocity measured by DVL-aided INS and relative velocities estimated by AUV model-based HGO along the x_i axis.

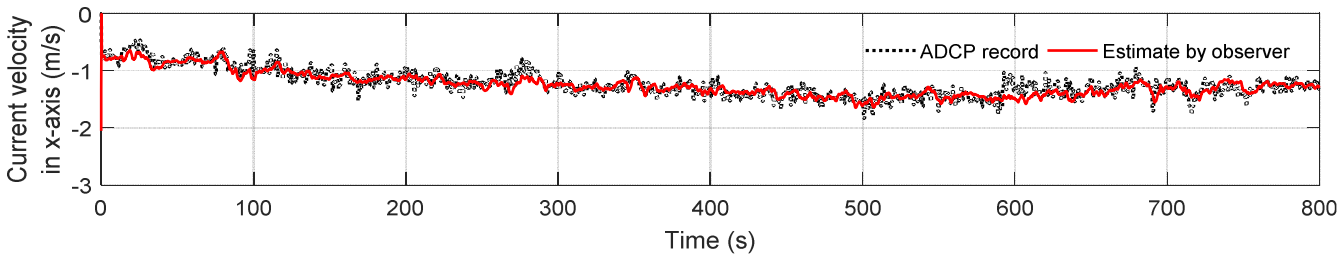

Fig. 10 The comparison between the current velocities measured by ADCP and its counterpart which was estimated by the HGO in the x_i axis

IV. CONCLUSIONS

In this paper, the water current velocity components in the x_i, y_i and z_i axes of the inertial reference frame were estimated to verify the capability of an AUV dynamic model-based observer for predicting current velocities around the vehicle. The water current velocities were estimated by calculating the difference between the vehicle's absolute velocities over ground and the relative velocities through the water estimated from the AUV model-based HGO.

The nonlinear observer for current estimation based on the AUV dynamic model proposed in reference [8] has been enhanced by having a high-gain. Stability of the estimation error dynamics was investigated via a Lyapunov function. The observer gain was computed by solving the LMIs which represented the error dynamics equation. In the numerical simulation, the vehicle's relative velocities were firstly estimated through the HGO and then the current velocity was further calculated by subtracting the vehicle's relative velocities from the absolute velocities. The estimated current velocities were well matched with the actual current velocities. The differences between the estimated and actual current velocities were quantified by calculating standard deviations as 0.0128 m/s, 0.0038 m/s and 0.0001 m/s for the x_i, y_i and z_i axes in inertial reference frame. The estimation error means of the HGO using the LMI have smaller values than using the pole placement method in both x_i and y_i axes which results in an estimation improvement of 45 % and 1% respectively. To validate the HGO, AUV field test was conducted a straight-line, constant altitude mission to record the current velocities and vehicle velocities by using an on-board ADCP and DVL respectively. The vehicle's relative velocities through the water were obtained by inserting equivalent control commands as were executed during the field tests. Once the vehicle velocities through water were available, the current velocities were calculated by subtracting the vehicle's relative velocities from the vehicle's absolute velocities recorded by the DVL-aided INS. The estimated current velocities x_i, y_i and z_i axes in the inertial reference frame were well matched with the measured current from the AUV-onboard ADCP. The differences between the estimated and measured current velocities were quantified using standard deviations as 0.0942 m/s, 0.0656 m/s and 0.0323 m/s.

For precise navigation and control of the AUV, it is critical to obtain the current velocities close to the AUV where the ADCP is unable to measure due to its blanking distance. Hence the AUV model-based high-gain observer is advantageous to estimate the current velocities either close to or at the vehicle by utilising the AUV dynamics model with precise hydrodynamics properties identified from the on-line measurement.

REFERENCES

[1] L. Medagoda, S. B. Williams, O. Pizarro, and M. V. Jakuba, "Water column current aided localisation for significant horizontal trajectories with Autonomous Underwater Vehicles," in *OCEANS'11 MTS/IEEE KONA*, 2011, pp. 1-10.

[2] P. S. Randeni, A. L. Forrest, R. Cossu, Z. Q. Leong, D. Ranmuthugala, and V. Schmidt, "Parameter identification of a nonlinear model: replicating the motion response of an autonomous underwater vehicle for dynamic environments," *Nonlinear Dynamics,* journal article vol. 91, no. 2, pp. 1229-1247, January 01 2018.

[3] M. Dinc and C. Hajiyev, "Integration of navigation systems for autonomous underwater vehicles," *Journal of Marine Engineering & Technology,* vol. 14, no. 1, pp. 32-43, 2015/01/02 2015.

[4] O. Hegrenas, E. Berglund, and O. Hallingstad, "Model-aided inertial navigation for underwater vehicles," in *2008 IEEE International Conference on Robotics and Automation*, 2008, pp. 1069-1076.

[5] Ø. Hegrenaes and O. Hallingstad, "Model-Aided INS With Sea Current Estimation for Robust Underwater Navigation," *IEEE Journal of Oceanic Engineering,* vol. 36, no. 2, pp. 316-337, 2011.

[6] P. G. Thomasson, "Equations of Motion of a Vehicle in a Moving Fluid," *Journal of Aircraft,* vol. 37, no. 4, pp. 630-639, 2000/07/01 2000.

[7] C. Woolsey, "Vehicle Dynamics in Currents," Virginia Center for Autonomous Systems2011, Available: http://www.unmanned.vt.edu/discovery/reports/VaCAS_2011_01.pdf.

[8] S. Fan, W. Xu, Z. Chen, and F. Zhang, "Nonlinear observer design for current estimation based on underwater vehicle dynamic model," in *OCEANS 2016 - Shanghai*, 2016, pp. 1-5.

[9] J.-P. Gauthier and I. Kupka, *Deterministic observation theory and applications*. Cambridge university press, 2001.

[10] H. K. Khalil, "High-gain observers in nonlinear feedback control," in *2009 IEEE International Conference on Control and Automation*, 2009, pp. 1527-1528.

[11] A. Alessandri and A. Rossi, "Time-varying increasing-gain observers for nonlinear systems," *Automatica,* vol. 49, no. 9, pp. 2845-2852, 2013/09/01/ 2013.

[12] J. G. VanAntwerp and R. D. Braatz, "A tutorial on linear and bilinear matrix inequalities," *Journal of Process Control,* vol. 10, no. 4, pp. 363-385, 2000/08/01/ 2000.

[13] P. G. Thomasson, *Equations of Motion of a Vehicle in a Moving Fluid*. 2000, pp. 630-639.

[14] P. G. Thomasson and C. A. Woolsey, "Vehicle Motion in Currents," *IEEE Journal of Oceanic Engineering,* vol. 38, no. 2, pp. 226-242, 2013.

[15] S. Fan and C. A. Woolsey, "Underwater vehicle control and estimation in nonuniform currents," in *2013 American Control Conference*, 2013, pp. 1400-1405.

[16] A. Alessandri and A. Rossi, "Increasing-gain observers for nonlinear systems: Stability and design," *Automatica,* vol. 57, pp. 180-188, 2015/07/01/ 2015.

[17] MathWorks. (2018). *LMI Applications*. Available: https://au.mathworks.com/help/robust/ug/lmi-applications.html?searchHighlight=lmi&s_tid=doc_srchtitle

[18] E. Kim, S.Fan, and N.Bose, "Estimating Water Current Velocities by using a Model-Based High-Gain Observer for an Autonomous Underwater Vehicle " *IEEE Access,* 2018.

[19] T. Prestero, "Verification of a six-degree of freedom simulation model for the REMUS autonomous underwater vehicle," Master's Thesis, Massachusetts Institute of Technology. Dept. of Ocean Engineering., Massachusetts Institute of Technology, Massachusetts Institute of Technology, 2001.

[20] P. S. Randeni, A. Forrest, R. Cossu, Z. Leong, and D. Ranmuthugala, "Determining the Horizontal and Vertical Water Velocity Components of a Turbulent Water Column Using the Motion Response of an Autonomous Underwater Vehicle," *Journal of Marine Science and Engineering,* vol. 5, no. 3, p. 25, 2017.